Corrected Copy

Entergy Operations, Inc.
1340 Echelon Parkway
Jackson, MS 39213-8298
Tel 601 368 5758

Michael A. Krupa
Director
Nuclear Safety & Licensing

CNRO-2003-00048

September 26, 2003

U. S. Nuclear Regulatory Commission
Attn: Document Control Desk
Washington, DC 20555

SUBJECT: Entergy Operations, Inc.
Response to Requests for Additional Information Pertaining to Relaxation Requests to NRC Order EA-03-009 for In-Core Instrumentation Nozzles

Arkansas Nuclear One, Unit 2
Docket No. 50-368
License No. NPF-6

Waterford Steam Electric Station, Unit 3
Docket No. 50-382
License No. NPF-38

REFERENCES:

1. Entergy Operations, Inc. letter CNRO-2003-00035 to the NRC, dated September 3, 2003
2. Entergy Operations, Inc. letter CNRO-2003-00042 to the NRC, dated September 18, 2003
3. Entergy Operations, Inc. letter CNRO-2003-00046 to the NRC, dated September 24, 2003

Dear Sir or Madam:

In Reference #s 1 and 2, Entergy Operations, Inc. (Entergy) initially requested relaxation from Section IV.C(1)(b) of NRC Order EA-03-009 for Arkansas Nuclear One, Unit 2 (ANO-2) and Waterford Steam Electric Station, Unit 3 (Waterford 3) pertaining to the in-core instrumentation (ICI) nozzles.

In a telephone conversation with Entergy representatives held on September 24, 2003, the NRC staff raised two questions pertaining to the analysis method that supports the ANO-2 relaxation request as documented in Engineering Report M-EP-2003-003, Rev. 0 (Enclosure 2 of Reference #1). These questions and Entergy's responses are provided in the enclosure to this letter.

A101

In addition, Entergy has identified a typographical error in Reference #3, which pertains to the ANO-2 relaxation request. Specifically, on page 2 of 20, Section III.B states that the blind zone located at the bottom of the in-core instrumentation (ICI) nozzle varies from approximately 0.20 inch to 0.70 inch. The correct size of the blind zone varies from 0.20 inch to 0.50 inch rather than to 0.70 inch as stated. This information is repeated in Section IV.B.3 (page 6 of 20) and on Figure 5 (page 17 of 20). This correction has no impact on the technical information presented in the letter.

This letter contains no new commitments.

If you have any questions or require additional information, please contact Guy Davant at (601) 368-5756.

Sincerely,

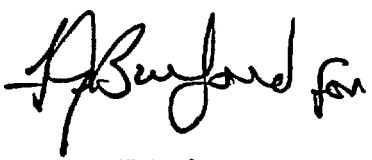

MAK/GHD/bal

Enclosure: Responses to the NRC's Request for Additional Information

cc: Mr. C. G. Anderson (ANO)
Mr. W. A. Eaton (ECH)
Mr. J. E. Venable (W3)
Mr. G. A. Williams (ECH)

Mr. T. W. Alexion, NRR Project Manager (ANO-2)
Mr. R. L. Bywater, NRC Senior Resident Inspector (ANO)
Mr. M. C. Hay, NRC Senior Resident Inspector (W3)
Mr. N. Kalyanam, NRR Project Manager (W3)
Mr. B. S. Mallett, NRC Region IV Regional Administrator

ENCLOSURE

CNRO-2003-00048

RESPONSES TO THE NRC'S
REQUEST FOR ADDITIONAL INFORMATION

RESPONSE TO THE NRC'S
REQUEST FOR ADDITIONAL INFORMATION

The NRC's questions and Entergy's responses as applied to analysis supporting ANO-2 Relaxation Request #3[1], as documented in Engineering Report M-EP-2003-003, Rev. 0 are provided below. Although raised during the review of the ANO-2 request, the questions and the methodology provided in the responses are also applicable to analysis supporting Waterford 3 Relaxation Request #3[2] since it employs the same method, as documented in Engineering Report M-EP-2003-005, Rev. 0. The numerical values provided in the responses below are specific to ANO-2; however, the values for Waterford 3, although different from the ANO-2 values, would not change the conclusions of the Waterford 3 analysis.

NRC Question 1:

It is stated in Section 3.1 of Enclosure 2 of your September 3, 2003 application [Entergy letter CNRO-2003-00035] that the counterbore was not explicitly modeled. This modeling is acceptable if the propagating crack tip is at some distance from the highly stressed area caused by the counterbore. However, for crack tips located within this highly stressed area such as Case 4 of your fracture mechanics analysis, you may need to evaluate the impact of the stress concentration factor (e.g., from Peterson's handbook) caused by the counterbore on the applied K calculation.

Response:

The Second Edition of Peterson's "Stress Concentration Factors" (Pilkey, 1997) does not explicitly provide solutions for counter-bored cylinders or internal shouldered or stepped cylinders. Similar references also yielded the same lack of explicit solutions for a cylindrical counterbore. A solution for an externally stepped hollow shaft would not be appropriate for the ICI nozzle geometry.

To address the explicit effect of a counterbore on the inside diameter (ID) of a cylinder (such as the ICI nozzle), several simplified finite element analysis (FEA) models were performed to quantify the relative impact of the counterbore on the applied stresses on the ICI nozzle. These stresses are used in the deterministic fracture mechanics evaluation of an axial surface flaw in the counterbore region. Two nozzle configuration models were evaluated:

(1) An ICI nozzle with a counterbore; and

(2) A straight cylinder with the thinnest section modeled the entire length.

Both cylinders had an outside diameter (OD) of 5.562 inch. The IDs of the counterbore models were 4.635 inches above the counterbore, and 4.760 inches below the counterbore; the straight cylinder model included a 4.760-inch ID. The counterbore was modeled 0.25 inch in length and 0.0625 inch in depth per ANO-2 design drawings

[1] Originally submitted via Entergy letter CNRO-2003-00035, dated September 12, 2003 and revised via Entergy letter CNRO-2003-00046, dated September 24, 2003.

[2] Originally submitted via Entergy letter CNRO-2003-00042, dated September 18, 2003 and revised via Entergy letter CNRO-2003-00045, dated September 24, 2003.

referenced in Engineering Report M-EP-2003-003. The axial spacing of the element mesh around the counterbore and the location where a counterbore would be in the straight cylinder model were refined to appropriately capture the stress distribution. Additionally, a total of 8 elements through the nozzle thickness were modeled.

The regions within the counterbore and below the counterbore were analyzed for applied stress. Specifically for the ANO-2 ICI geometry, using the design information in Section 2.0 of Engineering Report M-EP-2003-003, the location of the flaw tip for the most limiting flaw configuration (that is, Flaw Case 4, with a flaw spanning the 0.88-inch blind zone with a 6-to-1 length-to-depth aspect ratio) is approximately 0.3 inch below the bottom of the counterbore. These regions were evaluated for plausible stress concentrations resulting from the counterbore.

The flaw in the 0.88-inch blind zone is subject to membrane and bending residual + operating loads. To simulate the applied hoop loading conditions for which the axial flaw would be subject to and propagate in, two models for each nozzle configuration were constructed. The first set of models consisted of a unit (1000 psi) internal pressure load to simulate the contribution of the applied pressure loading in the nozzle and fixity applied on the OD at the bottom of the nozzle to simulate weld or head restraint. Figures 1a and 1b below show the two internal pressure models. The second set of models consisted of a horizontal unit force (1000 lb. or 1 kip) applied to the OD of the nozzle, with the top of the nozzle (away from the region of load application) fixed, to simulate the "hoop bending" effect caused by the J-groove weld residual stresses. This load condition will cause nozzle ovality, which is the primary cause of the hoop membrane and bending stresses in the nozzle. Figures 4a and 4b show the hoop bending load models.

The results of the finite element analyses are presented in the attached figures. Figures 2a and 2b show the applied hoop stresses for the internal pressure load case for the entire ICI nozzle model. A close-up of the hoop stresses in the vicinity of the counterbore and the bottom of the blind zone is shown in Figures 3a and 3b. The hoop bending load case hoop stresses for the entire models are shown in Figures 4a and 4b; a close-up of the counterbore and blind zone regions are shown in Figures 5a and 5b.

For both the internal pressure and hoop bending load cases, the existence of a circumferential counterbore has an insignificant impact on applied hoop stress. There is no appreciable increase in the hoop stress within and below the blind zone created by the counterbore.

A comparison of the hoop stresses between the two models was the primary focus on the FEA study. The presence of a circumferential counterbore in the ICI nozzle would serve to increase the axial stresses to some degree. To evaluate this increase, a set of models for the counterbore and straight nozzles was created that applied a unit axial stress (1000 psi) to the top of the nozzle and fixed at the bottom of the nozzle. An evaluation of the axial stress between the counterbore model and the straight nozzle model showed approximately a 30% increase in the axial stress magnitude in the counterbore model; no hoop stress effects occurred. If this simplified evaluation of an axial loading on the ICI nozzle is considered appropriate, then the axial stresses could be increased by a factor of 1.3. However, per Section 3.5 of Engineering Report M-EP-2003-003 (Enclosure 2 of Entergy letter CNRO-2003-00035), the circumferential stresses were predominantly compressive, with some low tensile (less than 6 ksi) stresses at the ID and quarter-point nodes. Using this simplified axial stress

concentration factor by multiplying the low tensile stress by a factor of 1.3, the resulting maximum axial stress would be 7.8 ksi. This value is still less than the 10 ksi stress above which circumferential flaw initiation could occur. Thus, this simplified factor used to augment the axial stress distribution does not change the conclusion that initiation of circumferential flaws in the 82° circumferential extent of the blind zone is precluded.

Figure 1a: Axisymmetric Counterbore Nozzle FEA model for Internal pressure

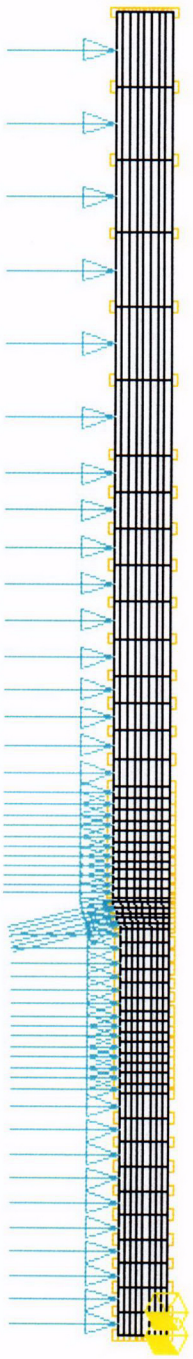

Dimensions:

OD = 5.562”

Upper ID = 4.635”

Lower ID = 4.760”

Counterbore height = 0.25”

Counterbore depth = 0.0625”

Distance from top of weld to bottom of counterbore ≈ 1.377”

Fixity (in all directions)

Figure 1b: Axisymmetric Straight Nozzle FEA model for Internal pressure

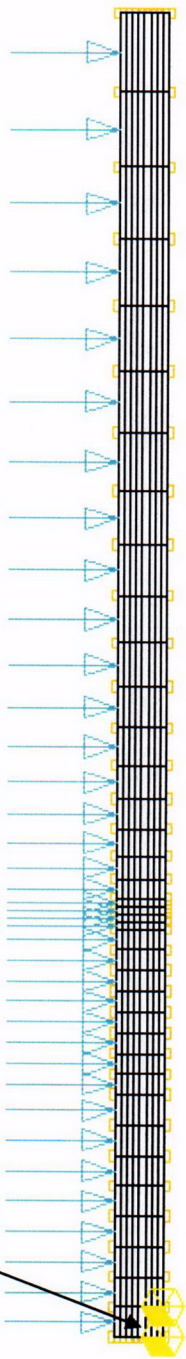

C01

Figures 2a and 2b: Counterbore Nozzle and Straight Nozzle Hoop Stress Plots for Internal pressure
(Stress in units of psi)

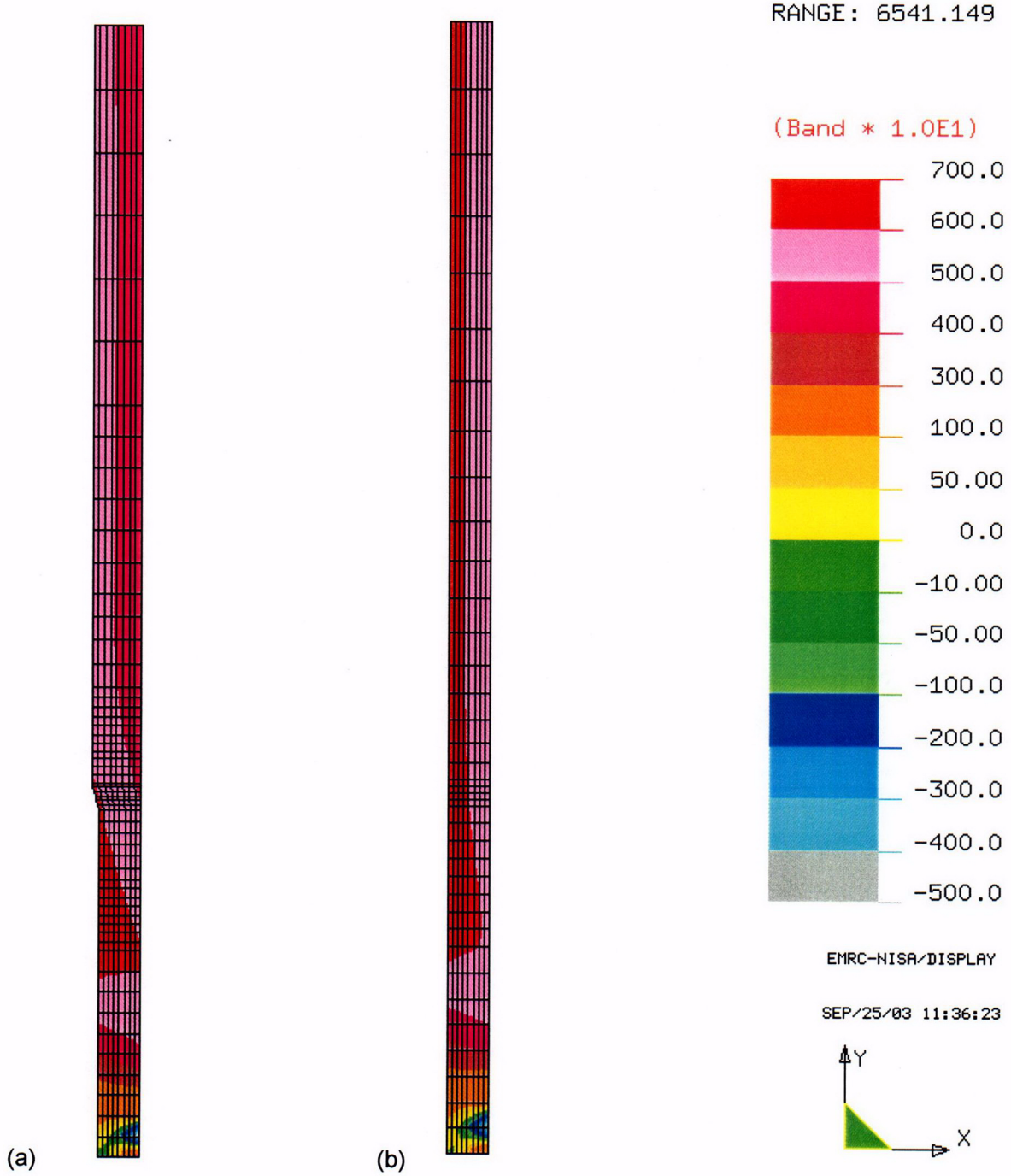

C02

Figure 3a: Counterbore Nozzle Hoop Stress Plots for Internal pressure—close-ups of blind zone region (Stress in units of psi)

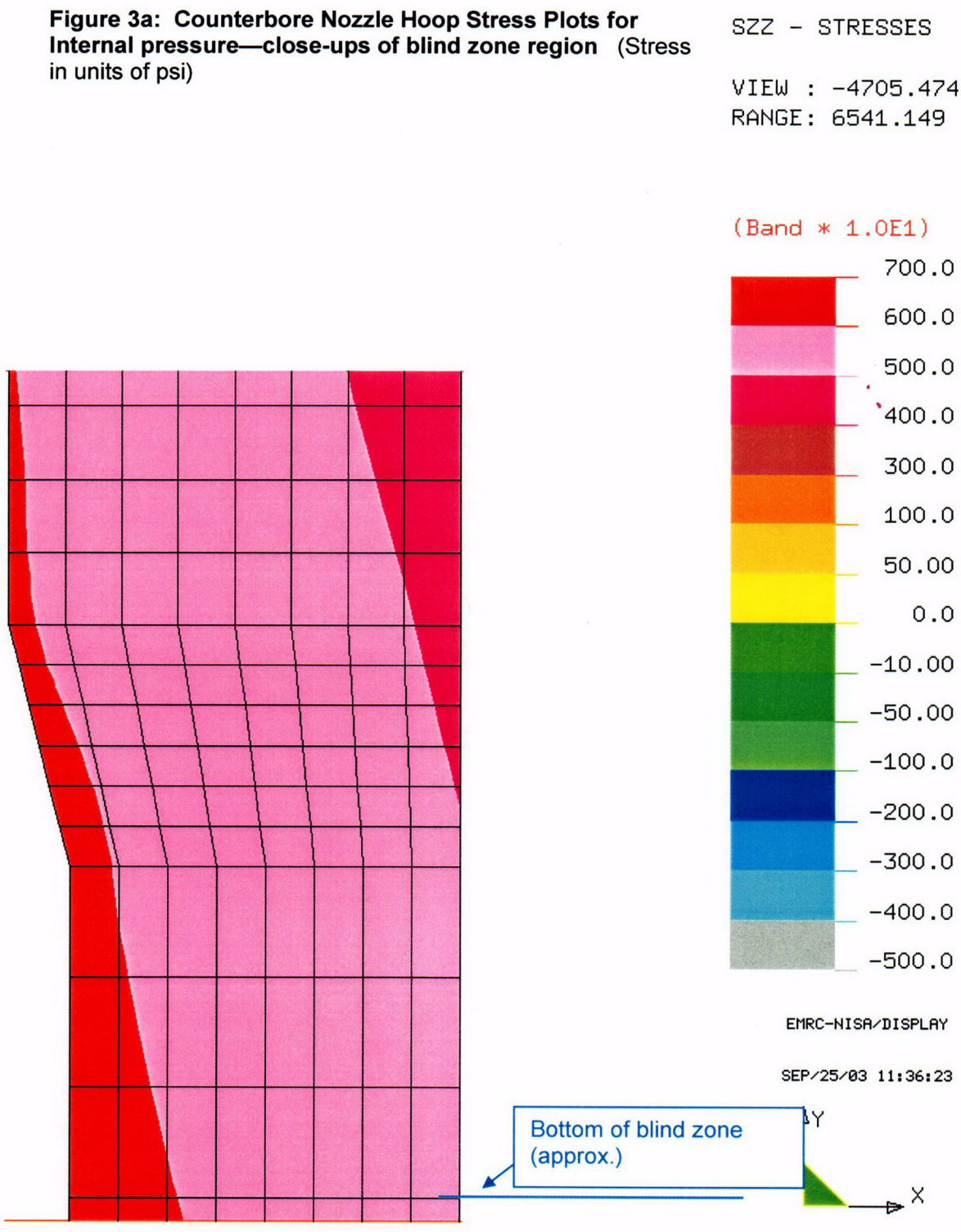

C03

Figure 3b: Straight Nozzle Hoop Stress Plots for Internal pressure—close-ups of blind zone region (Stress in units of psi)

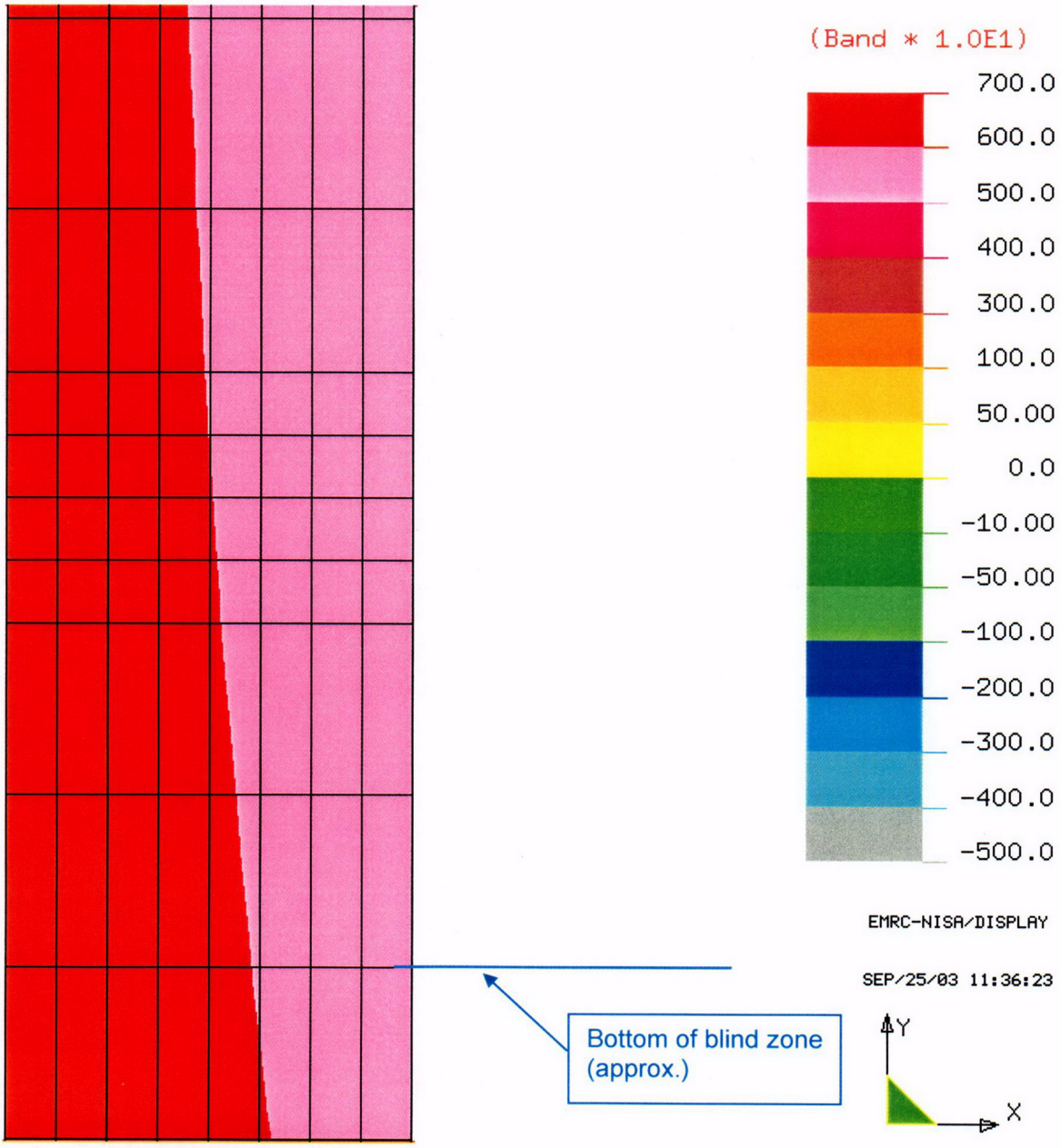

C04

Figure 4a: Counterbore Nozzle FEA model for Hoop Bending Load

Figure 4b: Straight Nozzle FEA model for Hoop Bending Load

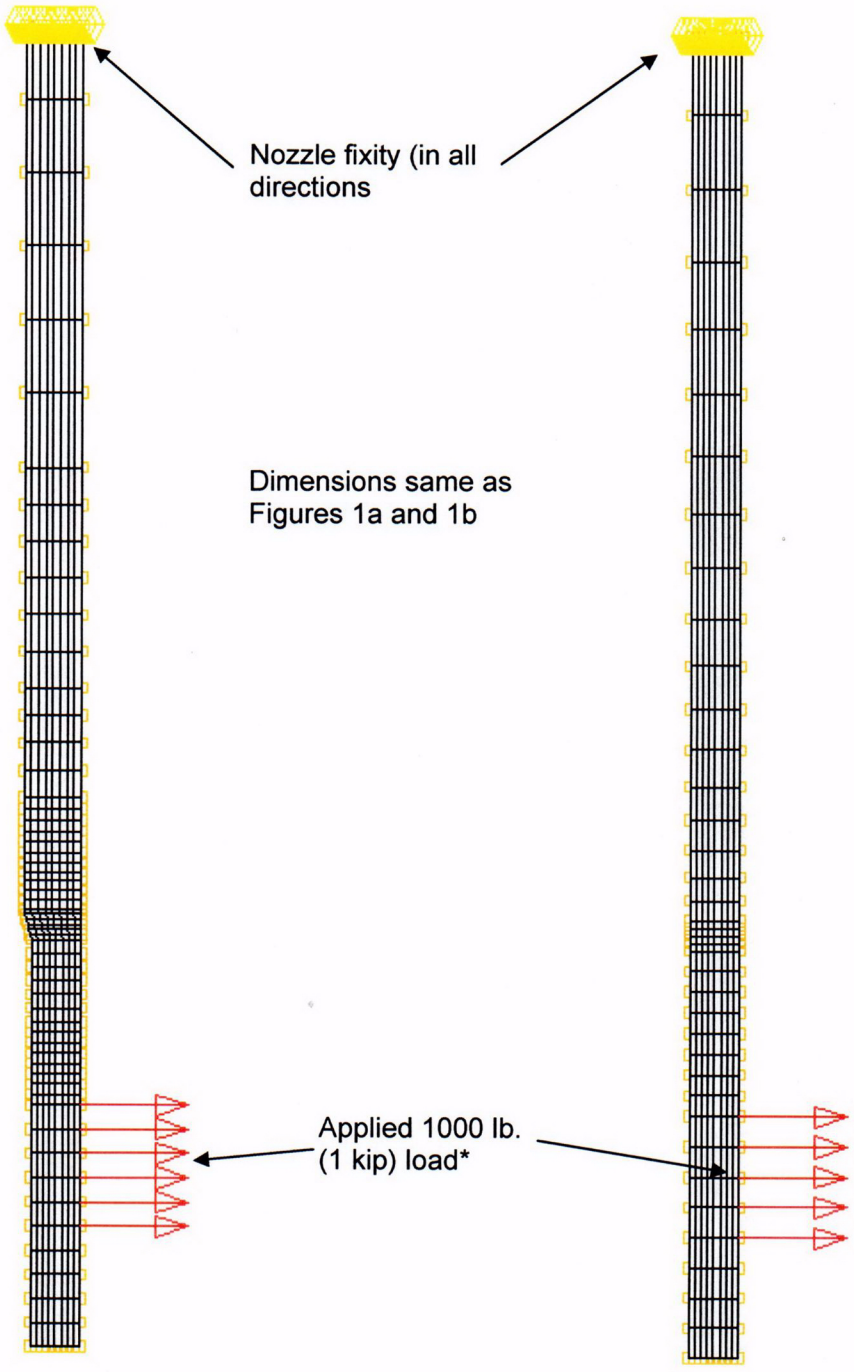

*Note that due to element spacing differences, the unit 1000 lb. load was applied over 6 nodes for the counterbore model and 5 nodes for the straight nozzle model.

C05

Figures 5a and 5b: Counterbore Nozzle and Straight Nozzle Hoop Stress Plots for Hoop Bending Load
(Stress in units of psi)

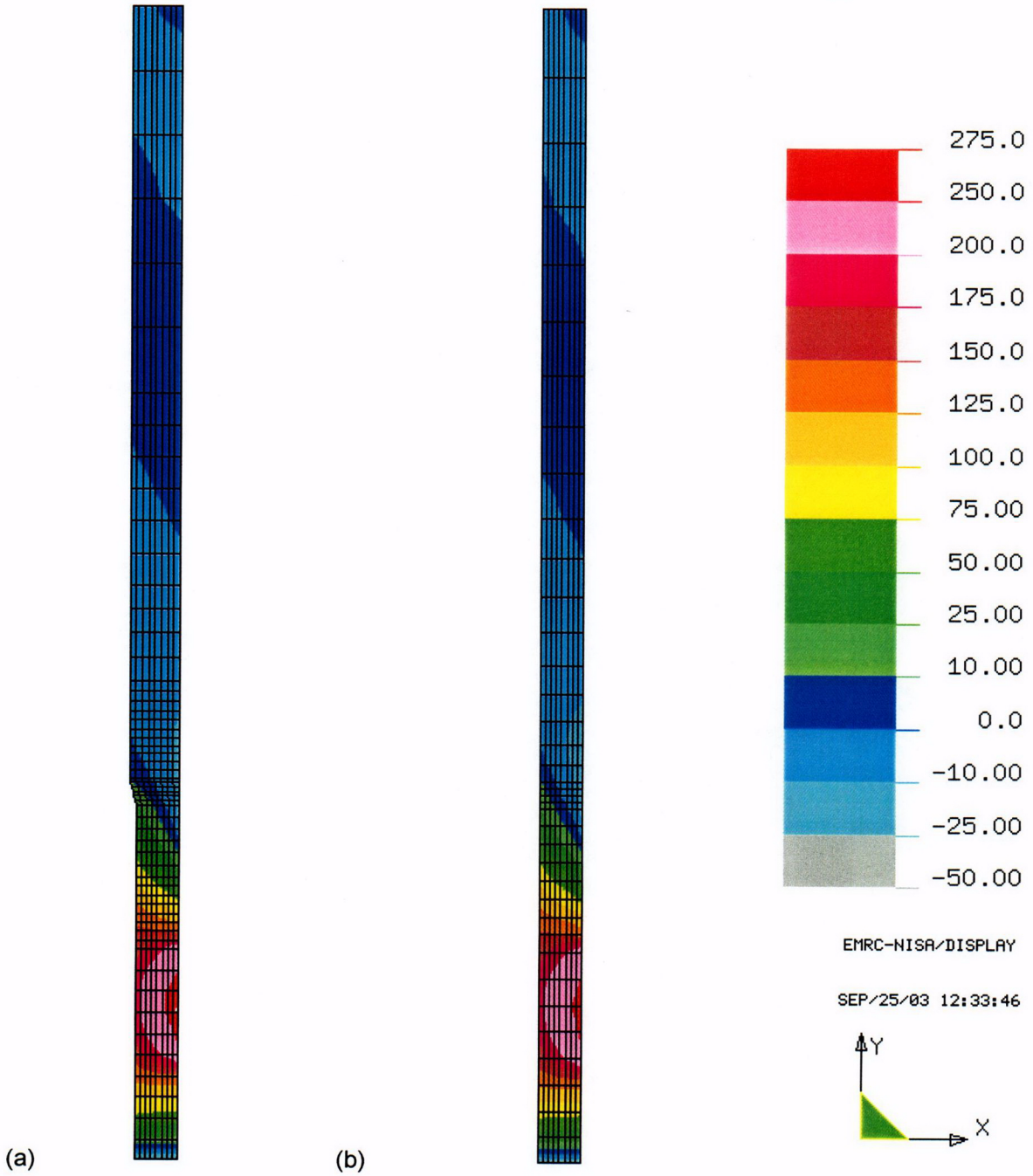

COC

Figure 6a: Counterbore Nozzle Hoop Stress Plots for Hoop Bending Load—close-ups of blind zone region
(Stress in units of psi)

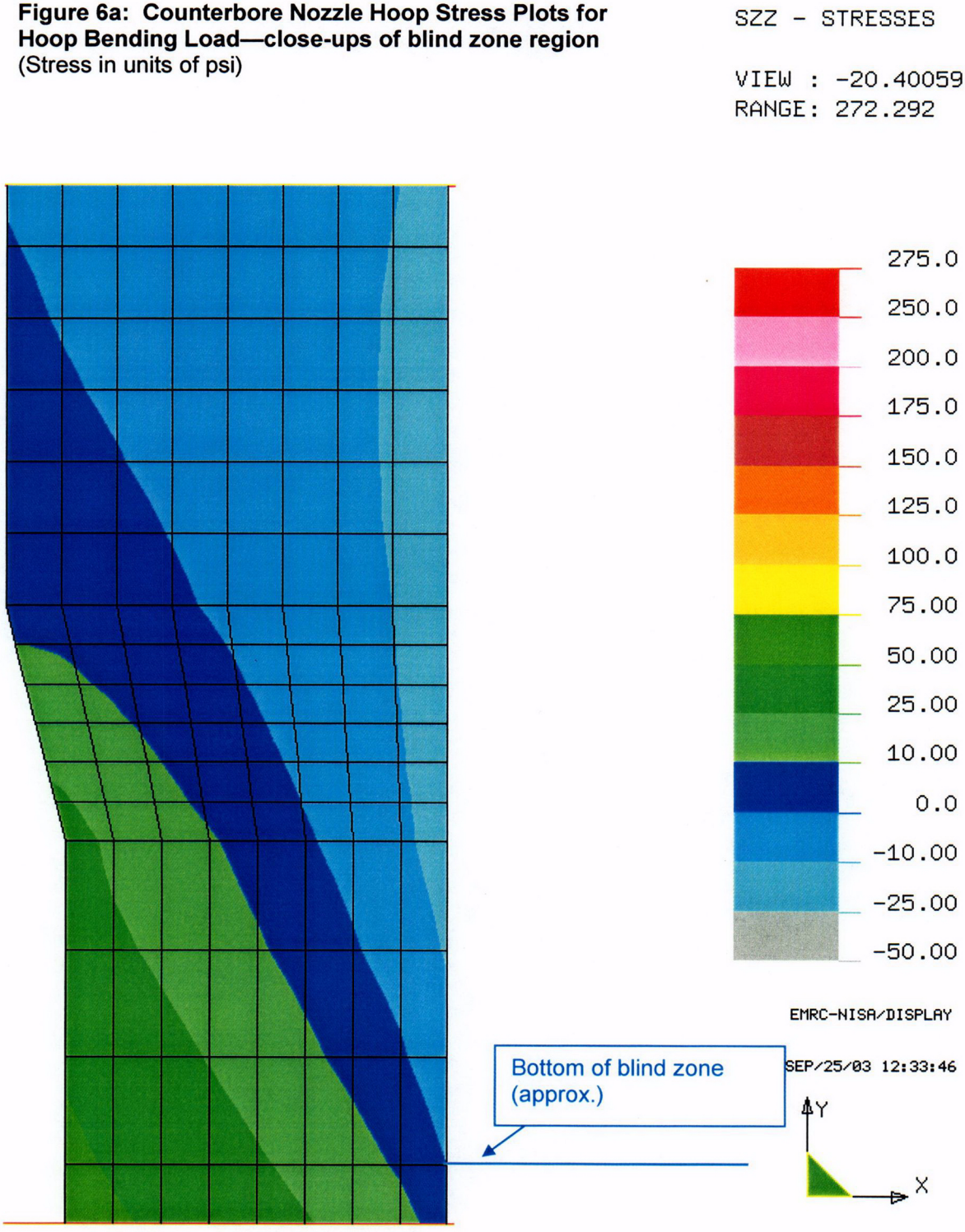

C07

Figure 6b: Straight Nozzle Hoop Stress Plots for Hoop Bending Load—close-ups of blind zone region (Stress in units of psi)

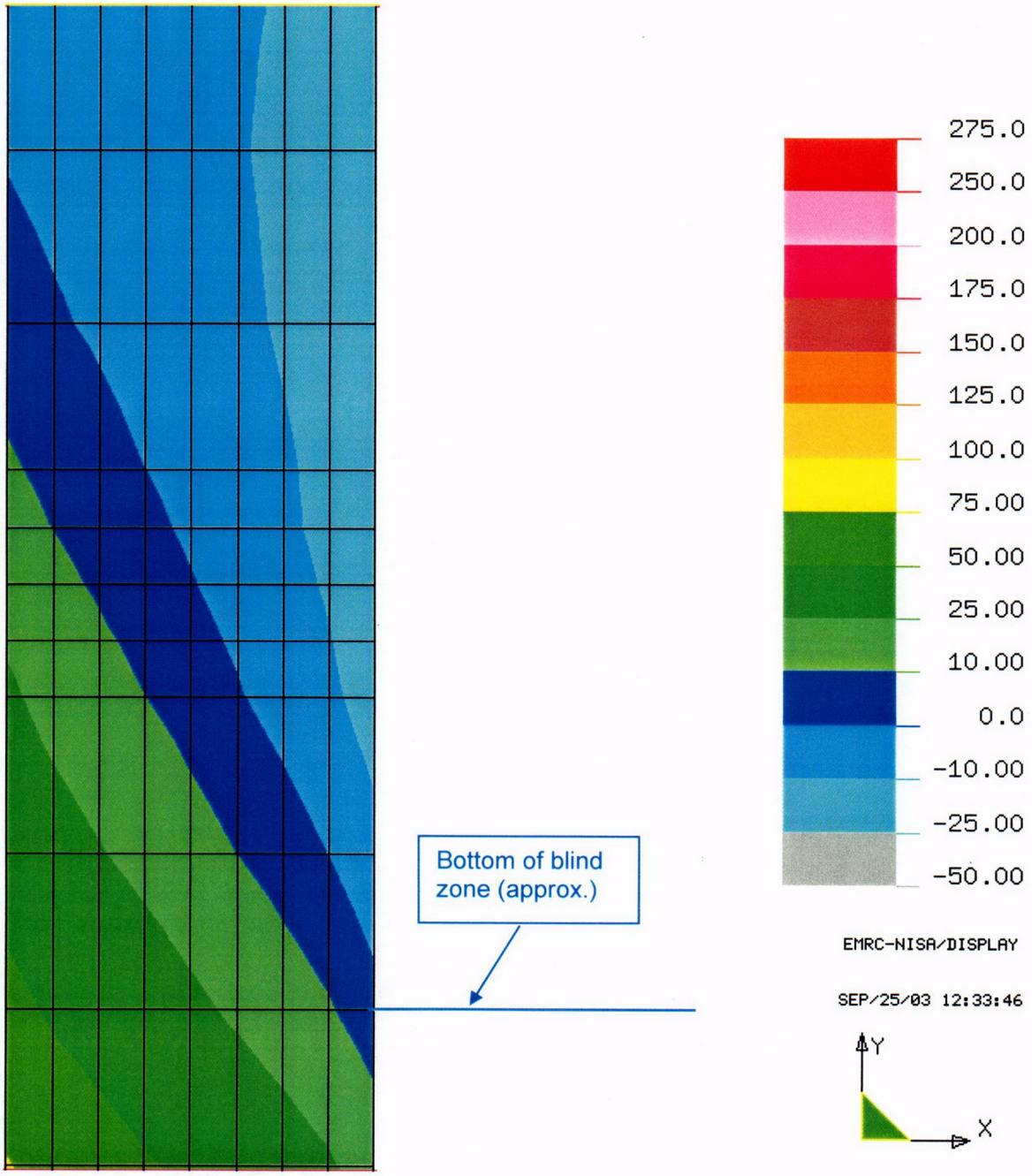

C08

NRC Question 2:

The applied K calculation for inside diameter (ID) surface flaws employed the "moving average scheme," which was also used in the fracture mechanics analyses for ID and outside diameter (OD) surface flaws for control element drive mechanism (CEDM) nozzles. An error analysis of this scheme is not necessary in the CEDM nozzles application because the results for the corresponding through-wall flaws are limiting with only one exception, and this exception is due to your approach of assuming the upper crack front for an initial OD or ID flaw to be 0.16 inch ahead of a corresponding through-wall flaw. In the in-core instrumentation (ICI) application, since the ID surface flaw is the only concern, a quantitative error analysis is required. One way to estimate the error is to find the ratio between the applied K for a crack with a concentrated opening force acting close to the crack tip and that for a crack with your average opening stresses. The concentrated force represents the difference between the stresses in the moving segments and the average stress.

Response:

The evaluation to determine the error by using the moving average stress for determining the stress intensity factor (SIF) followed the guidance provided in the NRC's question. The stress distribution considered for this evaluation was the ID surface stress in the counterbore region. The finite element analysis (FEA) nodal hoop stresses for the ID surface were fit with a third order polynomial. The curve representing the stress distribution is shown in Figure 1. In this figure the top and bottom of the blind zone together with the location of the counterbore are provided. The postulated crack encompasses the entire blind zone and is 0.88 inch long.

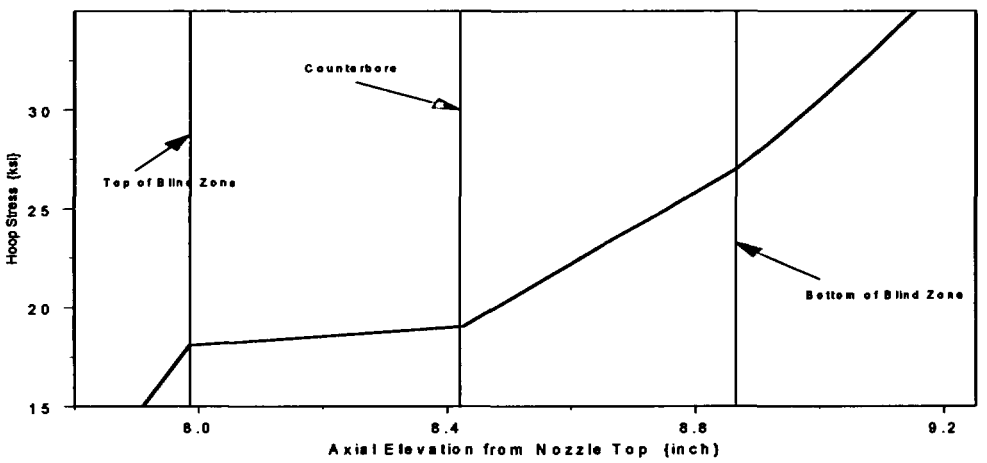

Figure 1: *Stress distribution used for analyses obtained from ICI FEA analysis. The stresses are on the ID surface of the ICI in the vicinity of the counterbore to top of the weld. The counterbore, the top and bottom of the blind zone are shown by the red and magenta lines respectively. The postulated crack encompasses the entire blind zone (the distance between the top and the bottom of the blind zone). Initial crack length was 0.88 inch. Crack propagation is towards the weld, which is to the right of the bottom of the blind zone line. The crack tip of interest is at the bottom of the blind zone.*

The model to estimate the SIF at the crack tip of interest, located at the bottom of the blind zone, used the concentrated force model of Reference 1. In this model a concentrated force (wedge force) is applied some distance (x) from the center of the crack. The equation for SIF for the crack tip at the bottom of the blind zone is given as:

$$K_I = \frac{P}{\sqrt{\pi a}}\sqrt{\frac{a+x}{a-x}}$$

where:

K_I = SIF at crack tip closest to applied force
P = Concentrated force (per unit thickness) or Wedge force
a = Half crack length
x = Distance from center of crack to point of applied concentrated force

The model for calculating the SIF using the stress obtained from the moving average method was a center cracked panel (CCP) such that a common geometry was used. The equation for the SIF is given by:

$$K_I = \sigma\sqrt{\pi a}$$

where:

K_I = SIF
σ = Applied stress obtained from the moving average technique
a = Half crack length

The stresses used to calculate the force used in the wedge crack model were from the stress distribution shown in Figure 1, whereas the stresses used for the CCP model were the moving average stresses obtained using the formulation described in Engineering Report M-EP-2003-003 (Enclosure 2 of Entergy letter CNRO-2003-00035). It is recognized that since the assumed crack encompasses the entire blind zone, the crack tip at the top of the blind zone is at a considerably lower stress. Hence, the average stress applied to the crack would be lower than the stress prevailing at the crack tip located close to the bottom of the blind zone. The wedge force was applied at the location of the initial crack tip (for the first iteration) and the half crack length was 0.458 inch. The wedge force model would provide the incremental SIF produced by the higher stresses at the crack tip at the bottom of the blind zone. The applied stress used for the CCP model was the average stress described above. Thus, the sum of the SIF from the two models would provide the prevailing SIF at the crack tip closest to the bottom of the blind zone. A ratio of the total SIF divided by the SIF obtained from the CCP model would provide the estimated error in the determination of the SIF using the model used in Engineering Report M-EP-2003-003.

A crack growth increment of 0.018 inch was used to perform the SIF calculations in an iterative manner. In the iterative calculation, the point of application of the wedge force was moved by the increment of crack growth as the half crack length was incremented. The SIF from the CCP model using the average stress was also calculated in an iterative manner using the same crack growth increment (0.018 inch). The SIFs from the two

models were summed at each crack growth increment to determine the total SIF. The results of the three SIFs determined are shown in Figure 2 below.

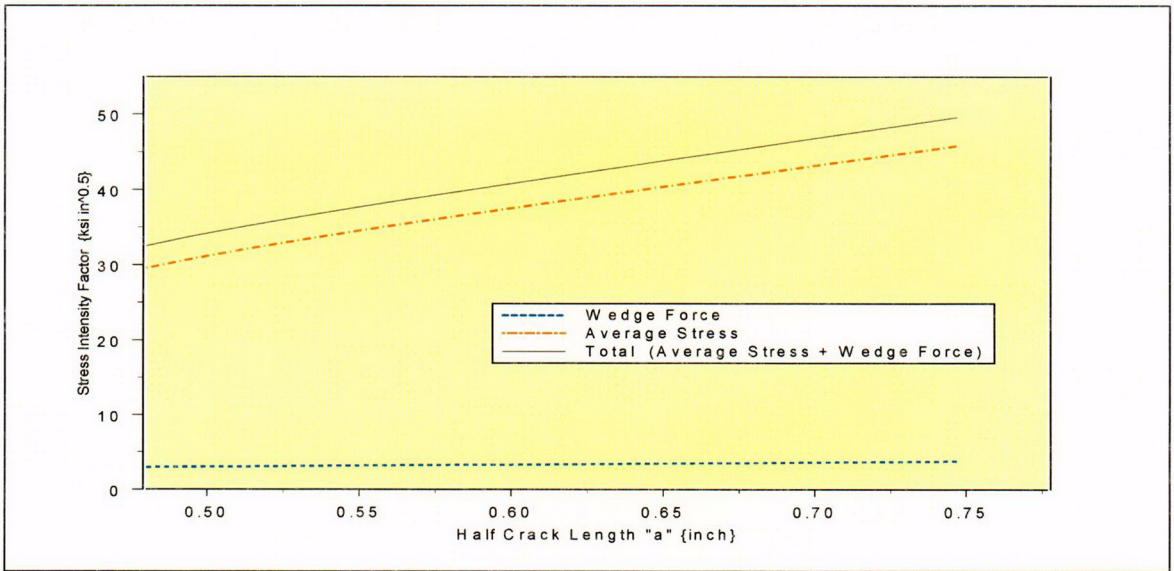

Figure 2: *The SIF for the wedge force is the lower curve. The SIF for the moving average method is the second curve from the bottom. The total SIF (moving average + wedge force) is the top curve.*

The iterative calculation was performed for fifty (50) increments. The mean value of the estimated SIF due to the wedge force was 8.53% of the SIF obtained by using the moving average stress (i.e., $K_{I,\ Wedge} = 0.0853 \times K_{I,moving\ average}$). This indicates that the SIF at the crack tip closest to the bottom of the blind zone may experience a higher SIF than that estimated using the moving average stress. To determine the error, the total SIF (sum of the SIF from the moving stress average method using the CCP model and the SIF from the wedge force model) was divided by the SIF obtained using the moving average stress and the CCP model. The resulting ratio would then be the effective error caused by the lower applied stress using the moving average stress. The mean ratio was estimated to be 1.0297, which implies an error of 2.97%.

Information provided in Reference 1 (page 357) indicates that the error in the estimation of SIF using an average stress, depending on the degree of non-uniformity of the actual stress distribution, would likely be less than 10%. This is borne out by the calculation performed and discussed above.

The models used in this analysis were for through-wall cracks using the ID stresses. Hence, the results of the analysis are applicable to the surface crack tip. Therefore, applying the results to the surface crack growth would suggest that there could be a slight increase in the crack growth along the ID surface. This would imply that the potential for detection of the postulated crack before reaching a through-wall condition would increase. In summary, the evaluation discussed above demonstrates that the salient conclusion made in Engineering Report M-EP- 2003-003 (i.e., there exists sufficient operating time margin to detect the postulated crack as it propagates outside the blind zone before reaching a through-wall condition) remains valid.

C09

Reference:

1. "Elementary Engineering Fracture Mechanics"; Fourth Edition; David Broek; Martinus Nijhoff Publishers; 1986

Reference:

1. "Elementary Engineering Fracture Mechanics"; Fourth Edition; David Broek; Martinus Nijhoff Publishers; 1986